

Interlayer Structure and Molecular Environment of Alkylammonium Layered Silicates

Richard A. Vaia, Rachel K. Teukolsky, and Emmanuel P. Giannelis*

Department of Materials Science and Engineering, Cornell University,
Ithaca, New York 14853

Received March 2, 1994. Revised Manuscript Received April 25, 1994*

Transmission Fourier transform infrared spectroscopy (FTIR) was used to probe the interlayer structure and phase state of intercalated alkylammonium silicates by monitoring frequency shifts of the CH₂ stretching and scissoring vibrations as a function of interlayer packing density, chain length, and temperature. A wide range of molecular environments varying from solidlike to liquidlike was found. In general, as the interlayer packing density or chain length decreases or the temperature increases, the chains adopt a more disordered, liquidlike structure. In intermediate cases, the chains are neither solidlike nor liquidlike but exhibit a liquid-crystalline character.

Introduction

Alkylammonium derivatives of mica-type layered silicates (MTS) are employed in a wide variety of industrial and scientific applications. Examples include rheological control agents in paints and greases,^{1,2} adsorbents for the treatment of contaminated waste streams,^{3,4} and models for studying chain aggregation in biomembranes.⁵ More recently, alkylammonium silicates have been used as artificial membranes,⁶ chemical sensors,^{7,8} host structures for direct melt intercalation of polymers,⁹ and reinforcements in polymer matrix composites.^{10,11} Last, they have been found to mediate the formation of mesoporous silicates.¹² In all of these applications, the behavior and properties of the hybrids depend largely on the structure and the molecular environment of the organic interlayer.

Traditionally, structural characterization has been limited to determining the orientation and arrangement of the alkyl chains based on X-ray diffraction analysis (XRD). Depending on the packing density, temperature, and chain length, the chains are thought to lie either parallel to the host layers forming lateral mono- or bilayers or radiate away from the surface forming extended (paraffin-type) mono- or bimolecular arrangements¹³⁻¹⁶

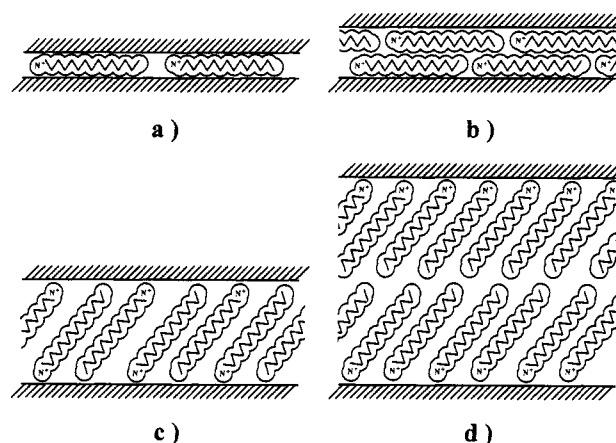


Figure 1. Alkyl chain aggregation in mica-type silicates: (a) lateral monolayer; (b) lateral bilayer; (c) paraffin-type monolayer; (d) paraffin-type bilayer. Adopted from ref 15.

(Figure 1). In some cases, individual chains are thought to adopt a hybrid arrangement with both lateral and paraffin-type segments leading to a pseudotrimer. Such idealized structures, based almost exclusively on *all-trans* segments are potentially misleading, since they fail to convey the most significant structural characteristic of aliphatic chains—the capacity to assume an enormous array of configurations because of the relatively small energy difference between *trans* and *gauche* conformers (0.6 kcal/mol, 2.5 kJ/mol).¹⁷

For illustrative purposes let us consider the case where the chains are thought to be in an extended (paraffin-type), tilted arrangement. An alternative arrangement based on a disordered chain configuration containing numerous *gauche* conformers would also be consistent with the observed gallery height (Figure 2). The different arrangements, however, although indistinguishable by X-ray, lead to much different interlayer structure and molecular environment. Determining the interlayer struc-

- * Abstract published in *Advance ACS Abstracts*, June 1, 1994.
 (1) Magauran, E. D.; Kieke, M. D.; Reichert, W. W.; Chiavoni, A. *NGLI Spokesman* 1987, 50, 453.
 (2) Mardis, W. S. *JAOCS* 1984, 61, 382.
 (3) Zielke, D. C.; Pinnavaia, T. J.; Mortland, M. M. In *Reactions and Movement of Organic Chemicals in Soils*, Soil Science Society of America and American Society of Agronomy: Madison, WI, 1989; pp 81-97.
 (4) Barrer, R. M. *Philos. Trans. R. Soc. London, A* 1984, 311, 333.
 (5) Lagaly, G. *Angew. Chem., Int. Ed. Engl.* 1976, 15, 575.
 (6) Okahata, Y.; Shimizu, A. *Langmuir* 1989, 5, 954.
 (7) Yan, Y.; Bein, T. *Chem. Mater.* 1993, 5, 905.
 (8) Russell, M. W.; Mehrotra, V.; Giannelis, E. P. In *Mater. Res. Soc. Symp. Proc.* 1991, 218, 153-158.
 (9) Vaia, R. A.; Ishii, H.; Giannelis, E. P. *Chem. Mater.* 1993, 5, 1694.
 (10) Usuki, A.; et al. *J. Mater. Res.* 1993, 8, 1179.
 (11) Yano, K.; et al. *J. Polym. Sci.: Part A, Polym. Chem.* 1993, 31, 2493.
 (12) Monnier, A.; Schüth, F.; Huo, Q.; Kumar, D.; Margolese, D.; Maxwell, R.; Stucky, G.; Krishnamurty, M.; Petrucci, P.; Firouzi, A.; Janicke, M.; Chmelka, B. *Science* 1993, 261, 1299.
 (13) Lagaly, G. *Clay Miner.* 1981, 16, 1-21.
 (14) Brindley, G. W.; Brown, G. *Crystal Structures of Clay Minerals and their X-Ray Identification*; Mineralogical Society, London, 1980; pp 226-230.
 (15) Lagaly, G. *Solid State Ionics* 1986, 22, 43.

- (16) Weiss, A. In *Proceedings of the Tenth National Conference on Clays and Clay Minerals*; Pergamon Press: New York, 1962; pp 191-224.
 Weiss, A. *Angew. Chem., Int. Ed.* 1963, 2, 134.
 (17) Flory, P. J. *Principles of Polymer Chemistry*; Cornell University Press: Ithaca, NY, 1953; pp 399-431.

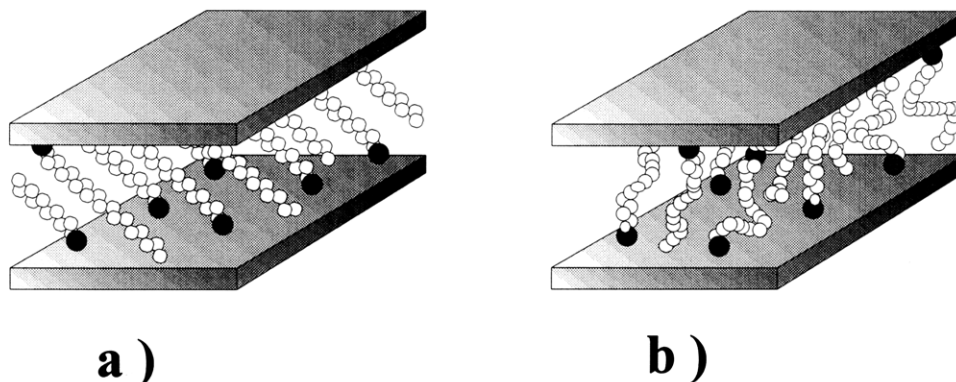


Figure 2. Different chain arrangements leading to the same gallery height: (a) tilted, *all-trans* chains and (b) chains with numerous *gauche* conformers. Open circles (O) represent CH₂ segments while cationic head groups are represented by filled circles (●).

ture solely on X-ray diffraction measurements is thus inadequate.

Investigators in many fields including colloidal and interface science,^{18,19} polymer science,²⁰ and biology²¹ have extensively used Fourier transform infrared spectroscopy (FTIR) to probe the structure and organization of molecules near interfaces and in colloids, aggregates, and bimolecular films. They have found that the frequency, width, height, and integrated intensity of the CH₂ and CH₃ infrared adsorption bands are sensitive to the *gauche/trans* conformer ratio of the chains as well as the intermolecular interactions between the chains.¹⁸ Thus they can be used to monitor structural rearrangements resulting from changes in packing density, temperature, pressure, and mechanical stress.^{18,22}

In this study, transmission FTIR is used in conjunction with XRD to probe the interlayer structure of intercalated alkylammonium silicates. Using various organically modified silicates, we have monitored the frequency shift of the asymmetric CH₂ stretching and scissoring vibrations as a function of interlayer packing density, chain length, and temperature. The FTIR measurements provide for the first time direct information on the structure of the organic interlayer as well as a means to relate the intercalated state to a corresponding bulk phase. The additional information garnered from these studies provide a more realistic description of the interlayer environment of the hybrids and could potentially improve our understanding of their properties.

Experimental Methods

Materials. Na⁺-montmorillonite with an exchange capacity of 80 mequiv/100 g (WM) was obtained from the University of Missouri Source Clay Repository (SWy-1). A higher exchange capacity Na⁺-montmorillonite (100 mequiv/100 g, SM) and Li⁺-fluorohectorite (150 mequiv/100 g, FH) were donated by Southern Clay Products, Inc., and Corning, Inc., respectively. Dioctadecyldimethyl ammonium bromide (2C₁₈N⁺2C₁Br⁻, Kodak) and a

series of primary alkyl amines (C_nH_{2n+1}NH₂, *n* = 6, 9, 10, 11, 12, 13, 14, 16, and 18, Aldrich Chemical) were used as received.

Synthesis. The organosilicate hybrids (FH-2C₁₈, SM-2C₁₈, WM-2C₁₈ and FH-C_n) were synthesized by a cation-exchange reaction between the layered silicates and excess alkylammonium salt (twice the exchange capacity of the host). The quaternary ammonium cation or the primary amine were dissolved in a 50:50 mixture of ethanol and deionized H₂O at 50–70 °C. In the case of primary amines an equivalent amount of HCl was also added to the solution. A 1 wt % aqueous suspension of the layered silicate was added to the alkylammonium solution and the mixture was stirred for 5–6 h at 50–70 °C. The cation-exchanged silicates were collected by filtration and subsequently washed with a mixture of hot ethanol and deionized H₂O until an AgNO₃ test indicated the absence of halide anions. The filter cake was dried at room temperature, ground, and further dried at 70–80 °C under vacuum for at least 24 h. The final powders were stored under vacuum with P₂O₅ desiccant.

Characterization. The interlayer packing densities were estimated thermogravimetrically (TGA) from the percent weight loss associated with decomposition of the interlayer organics. The analyses were carried out in air on a DuPont 951 Thermogravimetric analyzer at 10 °C/min. These results were selectively verified with elemental analysis (Galbraith Laboratories). The absence of either Cl or Br indicates that the hybrids are stoichiometric and contain no excess of alkylammonium ions.

FTIR spectra were collected using a Galaxy 2020 spectrometer with a nominal resolution of 4 cm⁻¹. Spectra were obtained from KBr pellets or films confined between two NaCl crystals mounted in a thermostatically controlled cell (Spectra Tech, Inc.). Care was taken to press all KBr pellets at the same conditions to minimize any effect of pressure on peak frequencies. Solution spectra in chloroform were obtained using a Perkin-Elmer demountable liquid cell. For each spectrum 64 interferograms were collected and coadded. Peak frequencies were determined using zero-point determination of the first derivative or center of gravity method and were reproducible with successive experiments to at least ±0.1 cm⁻¹.²³

XRD spectra were collected on a Scintag Inc. θ - θ diffractometer equipped with an intrinsic germanium detector system using either CuK α or CrK α radiation. Differential scanning calorimetry (DSC) was performed using a TA Instruments cell at 10 °C/min under N₂.

Results and Discussion

Effect of Packing Density. The effect of packing density on the interlayer structure was examined by intercalating dioctadecyldimethyl ammonium (2C₁₈) into WM, SM, and FH. As expected the interlayer packing density parallels the exchange capacity of the host increasing from WM to FH (Table 1). X-ray diffraction patterns of the hybrids show several harmonics with a

(18) Scheuing, D. R. In *Fourier Transform Infrared Spectroscopy in Colloid and Interface Science*; Scheuing, D. R., Ed.; ACS Symposium Ser. 447; American Chemical Society: Washington, DC, 1990; pp 1–21.

(19) Dluhy, R. A.; Cornell, D. G. In *Fourier Transform Infrared Spectroscopy in Colloid and Interface Science*; Scheuing, D. R., Ed.; ACS Symposium Ser. 447; American Chemical Society: Washington, DC, 1990; pp 192–207.

(20) Hagemann, H.; Snyder, R. G.; Peacock, A. J.; Mandlekern, L. *Macromolecules* **1989**, *22*, 3600.

(21) Dluhy, R. A.; Reilly, K. E.; Hunt, R. D.; Mitchell, M. L.; Mautone, A. J.; Mendelsohn, R. *Biophys. J.* **1989**, *56*, 1173.

(22) Wong, P. T. T.; Chagwedera, T. E.; Mantsch, H. H. *J. Mol. Struct.* **1991**, *247*, 31.

(23) Cameron, D. G.; Kauppinen, J. K.; Moffatt, D. J.; Mantsch, H. H. *Appl. Spectrosc.* **1982**, *36*, 245.

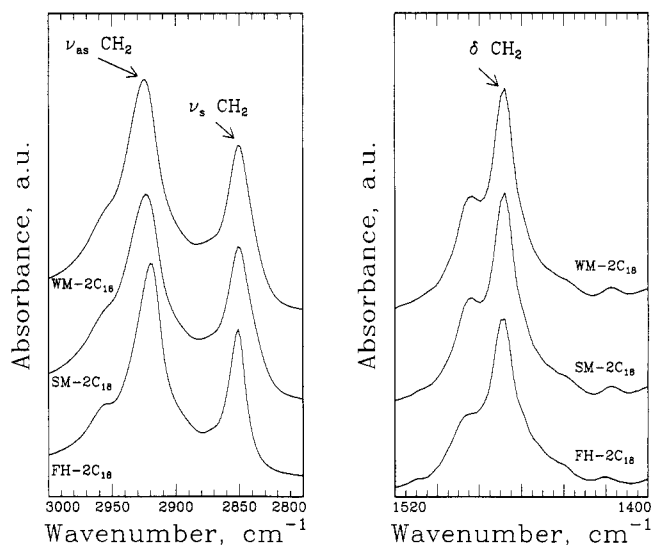


Figure 3. Selected regions of FTIR absorbance spectra of WM-2C₁₈, SM-2C₁₈, and FH-2C₁₈ hybrids displaying various methyl and methylene modes. The spectra were obtained at room temperature.

Table 1. Summary of XRD and FTIR Data for MTS-2C₁₈ Hybrids

	WM-2C ₁₈	SM-2C ₁₈	FH-2C ₁₈
aliphatic ions/Si ₃ O ₂₀ unit	0.65	0.80	1.2
gallery height (nm) ^a	1.43	1.57	2.85
layer area/molecule (nm ²)	0.72	0.58	0.39
layer area/chain (nm ²)	0.36	0.29	0.20
ν_{as} , CH ₂ (cm ⁻¹) ^b	2924.7	2923.6	2919.6
δ , CH ₂ (cm ⁻¹) ^b	1468.1	1468.3	1468.9

^a d_{001} - 0.95 nm (host layer thickness). ^b The FTIR spectra were obtained at room temperature.

primary repeat unit, d_{001} , of 2.38, 2.52, and 3.80 nm for WM-2C₁₈, SM-2C₁₈, and FH-2C₁₈, respectively.

To directly probe the molecular conformation of the intercalated chains and provide a better insight to the interlayer structure, FTIR spectroscopy was used. The strongest aliphatic absorption bands observed in the MTS-2C₁₈ hybrids are the methylene modes between 3000 and 2800 cm⁻¹ and between 1520 and 1400 cm⁻¹ (Figure 3). The bands at ~2920 and 2850 cm⁻¹ arise from the CH₂ asymmetric, ν_{as} (CH₂), and symmetric, ν_s (CH₂), stretch, respectively. The band around 1470 cm⁻¹ is due to the CH₂ bending (scissoring) vibration, δ (CH₂).²⁴ The peak frequency of these modes along with packing density, gallery height, and area available per guest molecule for WM-2C₁₈, SM-2C₁₈, and FH-2C₁₈ are summarized in Table 1.

As the interlayer packing density increases, ν_{as} (CH₂) shifts from 2924.7 to 2923.6 to 2919.6 cm⁻¹ for WM-2C₁₈, SM-2C₁₈, and FH-2C₁₈, respectively. Even though the frequency shifts appear to be relatively small, they are rather significant considering that they are reproducible to a least ± 0.1 cm⁻¹. In general, the frequency and width of ν_{as} (CH₂) are sensitive to the *gauche/trans* conformer ratio and the packing density of methylene chains.²⁵⁻²⁹ The band shifts from lower frequencies, characteristic of

highly ordered *all-trans* conformations, to higher frequencies and increased widths as the number of *gauche* conformations along the hydrocarbon chain (chain disorder) increases.²⁸ For example, the methylene chains in the *all-trans* ordered state of crystalline 2C₁₈N⁺2C₁Br⁻ exhibit a band at 2917.8 cm⁻¹. The band shifts to 2928.9 cm⁻¹ when the chains are in a liquidlike environment as in 2C₁₈N⁺2C₁Br⁻/CHCl₃ solution.

For FH-2C₁₈, an extended monolayer with chains normal to the layers or a tilted bilayer (Figure 1) are consistent with the measured gallery height. The proximity of ν_{as} (CH₂) to that observed for crystalline 2C₁₈N⁺2C₁Br⁻ indicates that a monolayer of predominantly extended, *all-trans* chains is present. In such a configuration there is a perfect match between the cross-sectional area of the extended molecules (0.40 nm²)³⁰ and the available area/guest molecule (0.39 nm²). The presence of extended chains normal to the surface is further supported by the observed gallery height (2.85 nm), which is also consistent with a monolayer of fully stretched chains (~2.6 nm^{31,32}). A bimolecular arrangement (Figure 1d) with fully stretched chains tilted 33° with respect to the surface seems unlikely, since the large area/molecule available (0.80 nm²) would favor a disordered configuration due to the tendency of the chains to maximize their conformational entropy, which would lead to much higher ν_{as} (CH₂) than observed.

As the chain packing density progressively decreases and the available surface area per guest molecule increases, the gallery height decreases to 1.57 and 1.43 nm in SM-2C₁₈ and WM-2C₁₈, respectively. The decrease in gallery height is accompanied by similar shifts in the ν_{as} (CH₂) to higher frequencies consistent with chains with increased *gauche* conformers. With decreasing packing density, the chains are no longer fully stretched in an *all-trans* conformation but they progressively adopt a more disordered structure (Figure 2b). Again, a tilting arrangement containing *all-trans* chains, although consistent with the XRD measurements, seems unlikely in view of the IR data.

Aggregation of chains into kink and *gauche* blocks containing *gauche* conformers has been previously proposed by Lagaly to account for the temperature dependence of gallery height in high-temperature phases of bimolecular paraffin-type hybrids.⁵ We assert that the presence of *gauche* conformations is more ubiquitous while *all-trans* segments are present only under special circumstances (i.e., when the cross-sectional area of the intercalated molecules is about the host area/guest molecule). Furthermore, to the best of our knowledge this is the first direct experimental confirmation for the presence of *gauche* segments in intercalated systems.

Using the frequency shifts as a guide, we can also determine the phase state of the interlayer. Increased

(26) Kawai, T.; Umemura, J.; Takenaka, T.; Kodama, M.; Seki, S. *J. Colloid Interface Sci.* **1985**, *103*, 56.

(27) Wang, W.; Li, L.; Xi, S. *J. Colloid Interface Sci.* **1993**, *155*, 369.

(28) Weers, J. G.; Scheuing, D. R. In *Fourier Transform Infrared Spectroscopy in Colloid and Interface Science*; Scheuing, D. R., Ed.; ACS Symposium Ser. 447; American Chemical Society: Washington, DC, 1990; pp 87-122.

(29) Cameron, D. G.; Umemura, J.; Wong, P. T. T.; Mantsch, H. H. *Colloids Surf.* **1982**, *4*, 131.

(30) Israelachvili, J. N. *Intermolecular and Surface Forces*; Academic Press: New York, 1992.

(31) Okuyama, K.; Soboi, Y.; Iijima, N.; Hirabayashi, K.; Kunitake, T.; Kajiyama, T. *Bull. Chem. Soc. Jpn.* **1988**, *61*, 1485.

(32) Okuyama, K.; Hoso, K.; Maki, N.; Hamatsu, H. *Thin Film Solids* **1991**, *203*, 161.

(24) In addition to the asymmetric and symmetric CH₂ stretching and CH₂ scissoring vibrations monitored in the present study, numerous other methylene and head group modes can be utilized in structural investigations of the tails of common end-functionalized aliphatic compounds.^{18,28} Many of these modes though were weak or masked by the silicate host.

(25) Snyder, R. G.; Strauss, H. L.; Elliger, C. A. *J. Phys. Chem.* **1982**, *86*, 5145.

chain order leads to more efficient packing and increased interchain contacts resulting in more cohesive van der Waals interactions between the chains and a greater interlayer solidlike character. Conversely, increased *gauche* conformations (increased disorder) leads to a more liquidlike state.¹⁹ On the basis of the CH₂ stretching band the chains in FH-2C₁₈ appear to be in a solidlike environment and become progressively more liquidlike in SM-2C₁₈ and WM-2C₁₈.

Additional structural and phase-state information may be gathered from the location and shape of the CH₂ bending mode, $\delta(\text{CH}_2)$. This band is sensitive to interchain interactions and the packing arrangement of the chains with frequencies ranging from 1466 to 1472 cm⁻¹.^{20,27-29} In general higher frequencies (~ 1472 cm⁻¹) indicate "ordering" of the methylene chains in an *all-trans* crystalline state. Conversely, lower frequency (~ 1466 cm⁻¹), band broadening, and decreasing intensity indicate a decrease in interchain interactions and an increase in chain motion which is normally associated with a liquid state.²⁸

All three MTS-2C₁₈ hybrids display an absorption between 1468 and 1469 cm⁻¹ with the lower frequency corresponding to the lower exchange capacity host (Figure 3, Table 1). Even at the lowest packing density (WM), we do not observe the broadening and decreased intensity associated with fully disordered, liquidlike chains.^{28,29} The observed absorption around 1468 cm⁻¹ is characteristic of a partially ordered phase where the chains are mobile while maintaining some orientational order.²⁸ A similar effect has been observed in the liquid-crystalline state of lipids, whose spectra also exhibit a band at 1468 cm⁻¹.²⁸

On the basis of the above, we suggest that even in the low packing density hosts (WM and SM) the interlayer is not completely disordered (liquidlike), but the chains retain some orientational order similar to that in a liquid-crystalline (LC) state. This assertion is further supported by the proximity of the $\nu_{\text{as}}(\text{CH}_2)$ for the two montmorillonites to that of liquid crystalline 2C₁₈N⁺2C₁Br⁻ (refs 31 and 32) (2923.8 cm⁻¹ at $T = 80$ °C) and not to the frequency characteristic of completely disordered chains of the same salt in solution (2928.9 cm⁻¹). Therefore, in contrast to bulk states of matter where the positional and orientational order of the molecules is solely dictated by the molecules themselves, the intercalated molecules retain some orientational order imposed by the physical presence of the silicate layers and the packing density requirements that maintain charge neutrality.

Effect of Chain Length. The dependence of interlayer structure on chain length has also been investigated. Figure 4 compares $\nu_{\text{as}}(\text{CH}_2)$ and gallery height for a series of organosilicate hybrids (FH-C_n) of varying alkyl chain length, C_n, but similar packing density. As the chain length increases, $\nu_{\text{as}}(\text{CH}_2)$ shifts stepwise from 2932 cm⁻¹ for FH-C₆ to 2921.1 cm⁻¹ for FH-C₁₈. The frequency shifts in $\nu_{\text{as}}(\text{CH}_2)$ are mirrored by similar step decreases in the gallery height (Figure 4) suggesting that they are interrelated.

On the basis of conventional models^{5,13-16} which relate the interlayer structure to chain length and packing density, we would predict a lateral monolayer for FH-C₆, lateral bilayer for FH-C₉ through FH-C₁₂ and eventually pseudotrilayer to paraffin-type for FH-C₁₃ to FH-C₁₈ (see Figure 1). The attractive interactions between the silicate surface and the intercalated molecules and the geometric constraining effect on these molecules most likely force

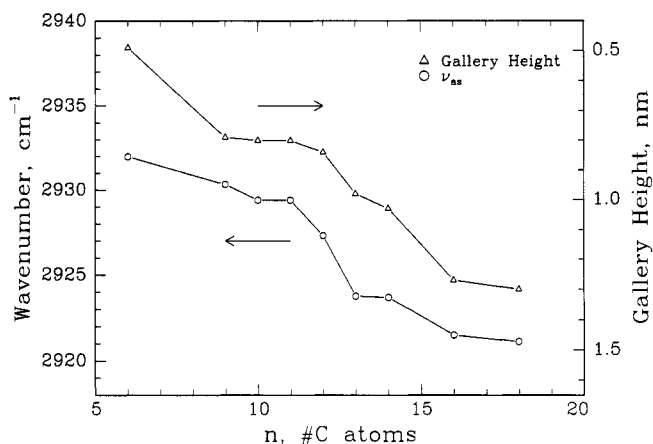


Figure 4. $\nu_{\text{as}}(\text{CH}_2)$ and gallery height as a function of chain length for FH-C_n measured at room temperature.

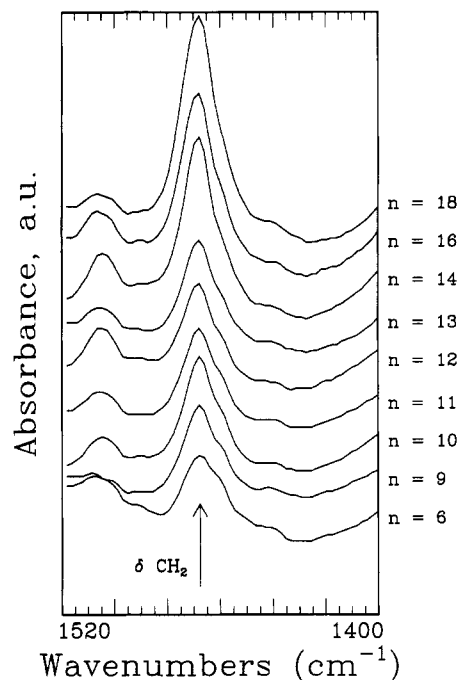


Figure 5. Room-temperature FTIR spectra for FH-C_n showing changes in the $\delta(\text{CH}_2)$ mode with decreasing chain length.

then to order in quasi-discrete layers.³⁰ The large variation in $\nu_{\text{as}}(\text{CH}_2)$ for the FH-C_n, however, suggests that the chains are in a wide range of molecular environments which is not obvious or implicit in the previously proposed idealized structures. Recall that shifts in the CH₂ stretching bands largely reflect changes in chain conformation, with the frequency shifting from lower frequencies for ordered, *all-trans* chains, to higher frequencies as the chain disorder (*gauche/trans* conformer ratio) increases. Conversely, interchain interactions dominate the CH₂ bending vibrations. Thus, if the chains in FH-C_n were to adopt the structures described above (see Figure 1), we would expect little variation in the CH₂ stretching frequencies in contrast to what we have observed.

By comparing the frequency of FH-C₁₈ to bulk C₁₈NH₃⁺Cl⁻, we find that the chains in the hybrid are in an LC state. This finding is consistent with our previous assignments, since the layer area/chain for both FH-C₁₈ (0.39 nm²) and WM-2C₁₈ (0.36 nm²) is similar and in the latter the chains are also in an LC state. Incidentally, the gallery height for the two hybrids is also comparable (1.33 and 1.43 nm for FH-C₁₈ and WM-2C₁₈, respectively). As

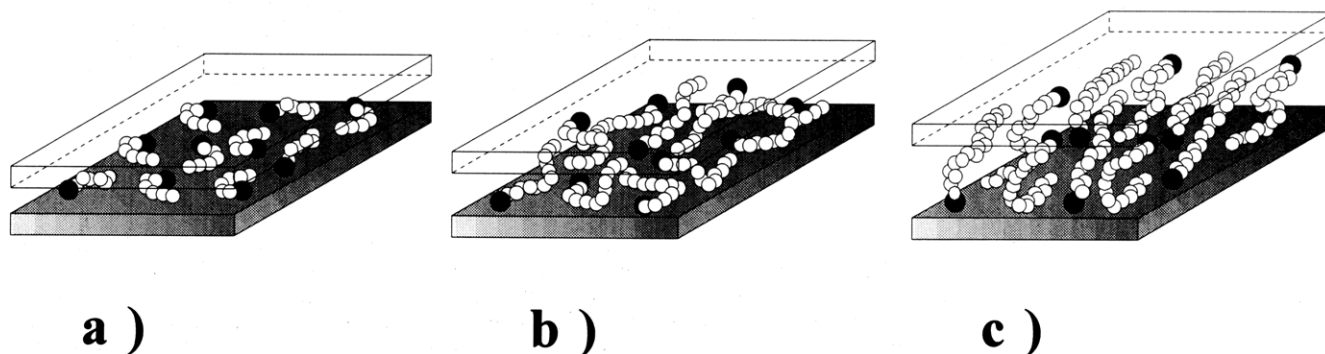


Figure 6. Alkyl chain aggregation models for FH- C_n . As the number of carbon atoms increases, the chains adopt a more ordered structure. For the shortest lengths (a), the molecules are effectively isolated from each other. At intermediate lengths (b), quasi-discrete layers form with various degrees of inplane disorder and interdigitation between the layers. For longer lengths (c), interlayer order increases leading to a LC environment. Open circles (○) represent CH_2 segments while cationic head groups are represented by filled circles (●). The top silicate layer has been left transparent to improve the perspective of the interlayer.

the chain length decreases and the available area per molecule increases the chains adopt a progressively more disordered structure and eventually become liquidlike for $n < 12$. In FH- C_6 , due to the short chain length, the chains are rather isolated such that the stretching frequency resembles that of chains in a gaseous state. The transition to a more liquidlike environment with decreasing chain length is further supported by decreasing intensity, peak broadening, and a shift to lower frequencies of the $\delta(\text{CH}_2)$ mode (Figure 5). A schematic representation of the proposed structures for the FH- C_n series is shown in Figure 6.

The proposed structures are consistent with recent molecular dynamic (MD) simulations of tethered and free alkane molecules either on free surfaces or confined between parallel plates. In general the physical presence of the impenetrable interface induces both normal and in-plane ordering of the chains.^{33–35} The fraction of *gauche* conformers, however, although generally less than that observed for the liquid alkanes (30%), is still quite substantial. In addition, some interdigitation of chain segments between those closest to the interface and subsequent layers has been observed. Of particular interest are simulations of C_8 alkane molecules tethered to a free silicate surface with an area comparable to the FH- C_n series (0.41 nm^2 per chain).³⁶ The simulations show that at room temperature the chain *gauche* conformer content is 30%, which is comparable to that of liquid alkanes and in excellent agreement with our assignment for $n < 12$.

Effect of Temperature. Last, the effect of temperature on the interlayer structure and phase state was examined. Figure 7 shows the temperature dependence of $\nu_{\text{as}}(\text{CH}_2)$ for FH- C_{18} . The respective behavior of WM- $2C_{18}$ is shown in Figure 8. In general, as the temperature increases the band shifts from that characteristic of the LC state to higher frequencies before it finally reaches a plateau with a frequency approaching that of a liquidlike state. The more disordered environment at elevated temperatures is further supported by peak broadening, decreasing intensity, and a shift to lower frequencies of the $\delta(\text{CH}_2)$ mode, as shown for FH- C_{18} in Figure 9. With

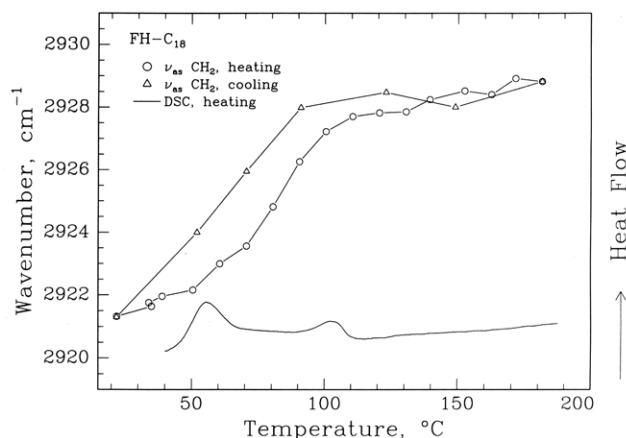


Figure 7. $\nu_{\text{as}}(\text{CH}_2)$ of FH- C_{18} as a function of temperature: (○) heating; (△) cooling. The corresponding DSC trace ($10 \text{ }^\circ\text{C}/\text{min}$ in N_2 ambient) is also included.

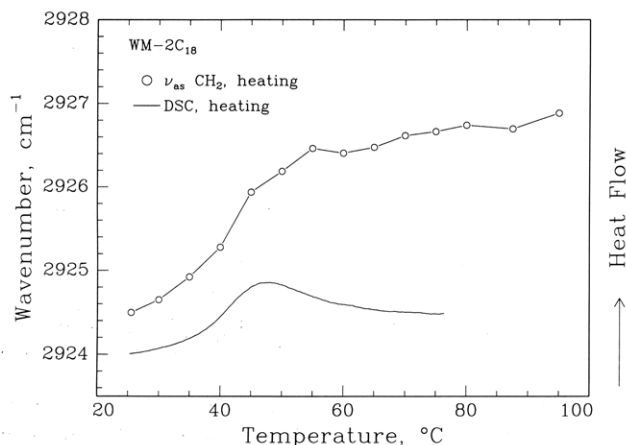


Figure 8. $\nu_{\text{as}}(\text{CH}_2)$ of WM- $2C_{18}$ as a function of temperature with the corresponding DSC trace ($10 \text{ }^\circ\text{C}/\text{min}$ in N_2 ambient).

increasingly elevated temperatures, successive degrees of disorder are introduced in the interlayer leading to a more liquidlike environment. The chain disordering on heating is consistent with MD simulations where the chains are shown to pass gradually from a low-temperature solidlike state to a high-temperature liquidlike state over a certain temperature range.³⁶

The interlayer transitions to a more disordered and eventually a liquidlike state are in very good agreement with the phase transitions observed in the DSC (Figures 7 and 8). The characteristic transitions in the FH- C_n series diminish in intensity and shift to lower temperatures with

(33) Xia, T. K.; Ouyang, J.; Ribarsky, M. W.; Landman, U. *Phys. Rev. Lett.* **1992**, *69*, 1967.

(34) Ribarsky, M. W.; Landman, U. *J. Chem. Phys.* **1992**, *97*, 1937.

(35) Vacatello, M.; Yoon, D.; Laskowski, B. *J. Chem. Phys.* **1990**, *93*, 779.

(36) Klatté, S. J.; Beck, T. L. *J. Phys. Chem.* **1993**, *97*, 5727.

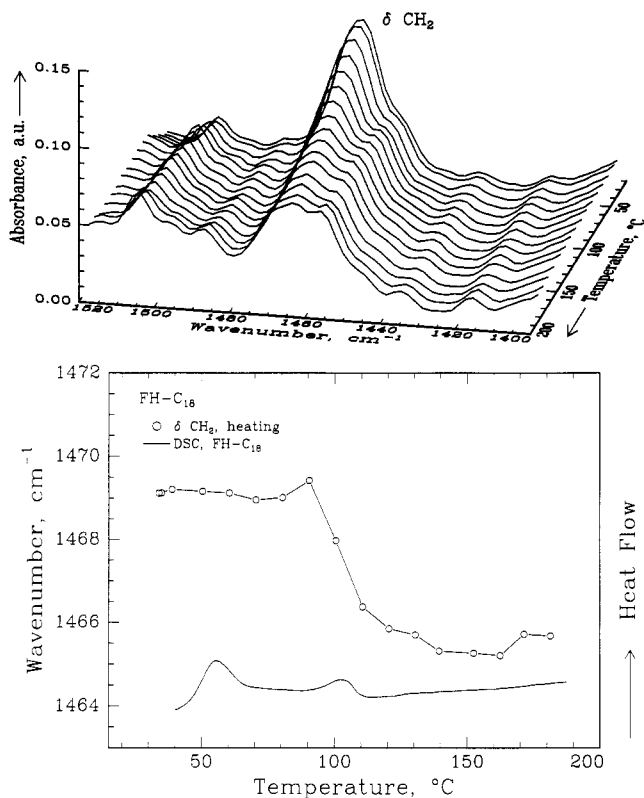


Figure 9. (a, top) FTIR spectra for FH-C₁₈ at different temperatures showing changes in the $\delta(\text{CH}_2)$ mode. (b, bottom) $\delta(\text{CH}_2)$ position as a function of temperature determined by the center of gravity method. The corresponding DSC trace (10 °C/min in N₂ ambient) is also included.

decreasing chain length indicating that the interlayer is already in a more liquidlike environment. In FH-C₁₈ both the IR and the DSC data suggest that there is a transition to another state before the chains adopt a completely disordered, liquidlike state.

The advantages of FTIR over XRD in probing the interlayer structure is evident by comparing changes in frequency and gallery height as a function of temperature. In contrast to the large frequency variation, which implies a wide range of interlayer environments, the gallery height changes very little over the same temperature range (Figure 10). At low temperatures the gallery height is virtually constant. Between 80 and 130 °C a modest increase of about ~0.08 nm is observed after which the gallery height plateaus out. The modest increase in the gallery height corresponds to the transition from solidlike to liquidlike environment.

The LC to liquidlike transition coincides with a dramatic increase in the capacitance of the hybrid.^{7,8} This behavior has been attributed to an increase in the interlayer fluidity, which is consistent with a transition to a more liquidlike environment observed in this study. Further evidence for the increased chain mobility comes from monitoring the $\nu_{\text{as}}(\text{CH}_2)$ during cooling (Figure 7). When the interlayer is liquidlike, the CH₂ frequency is practically identical during the heating or cooling cycles but becomes hysteretic on cooling below the liquidlike range. The chains become more sluggish as they adopt a more solidlike character preventing them from reaching instantaneously their equilibrium configuration, consistent with the MD simulations.³⁶

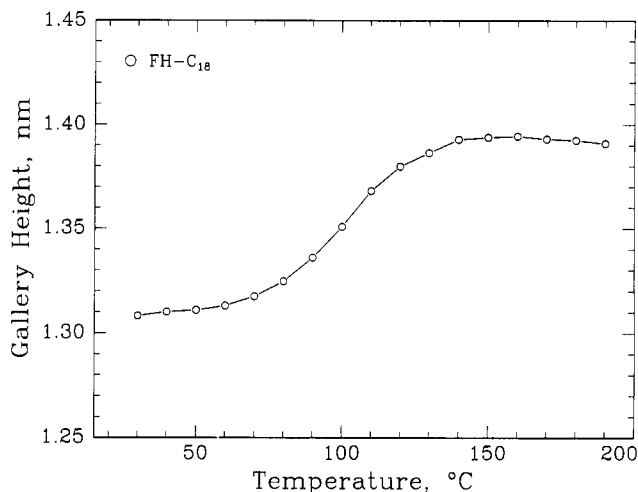


Figure 10. Temperature dependence of gallery height for FH-C₁₈.

Similar to the dielectric behavior, the state of the interlayer and the mobility of the chains are expected to control other properties of the hybrids. For example, while in the LC state the chains are expected to resist shear but flow and relax albeit at a slow rate. Furthermore, the interlayer environment will largely determine the adsorption and swelling characteristics of the hybrids. Experiments are currently underway to investigate the interlayer properties and correlate them with the structure and phase state.

Conclusions

In summary, FTIR spectroscopy in conjunction with X-ray diffraction studies have provided a new experimental insight into the interlayer structure and phase state of intercalated alkylammonium silicates. By monitoring frequency shifts of the asymmetric CH₂ stretching and bending vibrations, we have found that the intercalated chains exist in states with varying degrees of order. In general, as the interlayer packing density or the chain length decreases or the temperature increases, the intercalated chains adopt a more disordered, liquidlike structure resulting from an increase in the *gauche/trans* conformer ratio. When the available surface area/molecule is within a certain range, the chains are not completely disordered, but retain some orientational order similar to that in a liquid crystalline state. Since the chains are freer to move around and reorient in the liquidlike state, they can attain equilibrium configuration much faster compared to those in an LC or solidlike state. These findings differ from the proposed conventional models in which the chains adopt a static, *all-trans* configuration, with a fixed cross-sectional area.

Acknowledgment. This work was sponsored in part by AFOSR and Corning, Inc. and by generous gifts from Xerox and Southern Clay Products. R.A.V. is supported by a DoD Fellowship. R.K.T. was supported by an REU grant from Cornell University's Materials Science Center. We thank C. K. Ober for the use of equipment, H. Ishii for the C₁₈NH₃⁺Cl⁻ sample, and M. K. Chaudhury for many helpful discussions. This study benefitted from the use of MRL Central Facilities funded by the National Science Foundation.